29th Congress of the International Council of the Aeronautical Sciences
St. Petersburg, Russia; September 7-12, 2014

MISSION PROFILES ANALYSIS: GUIDELINES TO AIRCRAFT ACTUATORS NEW TECHNOLOGY SPECIFICATION

Aurélien Reysset*, Marc Budinger*, Jean-Charles Maré*
*** Université de Toulouse, INSA/UPS, Institut Clément Ader, Toulouse, 31077, France.**

Keywords: *electromechanical-actuator, specifications, models, mission profile analysis*

Abstract

The aim of the current paper is to propose innovative standard tools and models for new electromechanical actuators (EMAs) specifications release. This objective is motivated by a strong demand of the aeronautic industry especially to cut down development time and cost. The paper highlights new design drivers and limitations induced by such a technology and the challenges to rise. It explains how to take care of those imperfections, early, at requirements document writing phase, and how to integrate and test it into the aircraft loop. A Matlab-Simulink library, based on presented model, has been applied successfully on various examples of EMAs for primary flight control of an aircraft. It can be used as a help for specifications severity comparison and mission profile adaptation or data extraction.

1 Introduction

The current trend is to evolve toward more electrically operated aircraft in order to cut consuming non propulsive power and operation costs, to make power distribution networks lighter and highly reconfigurable. The electromechanical actuator, part of power-by-wire actuators, thus comes in as an alternative to today's servo hydraulic solution. Yet some barriers preventing such a technology from expanding persist: reliability issues especially while speaking about jamming, mass hardware materials still to be optimized and development/manufacturing/ testing costs which are still too elitist.

Therefore a great effort has been made as concerns the development of the technology at research level with European and National programs [1], to bring it to its final level of maturity. ACTUATION 2015 is one of them [2] and this report is part of the concepts developed within methods and tools standardization workpackage.

However, the technological step forward induces new challenges to face and new problems to handle. Indeed the preliminary design process such as the specifications phase cannot duplicate former practices and has to evolve. The reason is that electromechanical actuators inherit new limitations from their components such as thermal stress or rolling fatigue and complex coupling with the load to be controlled especially with high reflected inertia. Those topics were not addressed during hydraulic actuators development phase because these design drivers were not present. Specification consisted mostly in extreme working points and closed-loop dynamics constraints. Now, load and displacement transient history must be recorded as specific mission profiles and provided to the development teams. It will be shown here how they can be analyzed, simplified and transformed into a complete set of standard data. The advantages are numerous: first the aircraft maker does not disseminate his knowledge and the development and testing phase can be accelerated.

The proposed approach is implemented in a specification tool composed of a set of specific models which are presented in this communication.

2 The EMA and their design drivers

Nowadays aircrafts inboard a great number of actuating systems from primary [3] secondary flight control to service outlets (landing gear

extension/retraction, locking device…) covering a wide range of power.
All the mentioned application cases are likely to be equipped in the future by electromechanical actuators (EMAs).

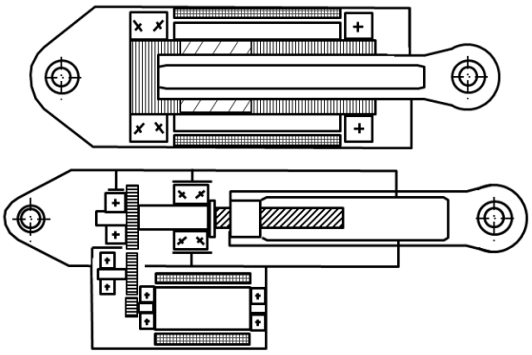

Figure 1: Direct drive vs. gear drive EMA

EMAs architectures present similarities, with power electronics, an electric motor, a mechanical transmission with balls/rollers-screw (linear actuator) and/or reducer (spur-gear, epicyclic, harmonic…), rod-ends, trust-bearing and housing for the whole package. The case studies developed in this paper will only be illustrated on both most common linear architectures presented in Figure 1: direct drive EMA [4] and parallel axis gear drive EMA [5].

EMAs architectures share components or are made of at least components subjected to the same kind of degradation phenomena and transient limitation. That is why it is interesting to list the so called "design drivers" which can, in some application cases, be relevant and drive the system design.

A distinction has to be made between rapid degradation leading to failure (transient limitations), and gradual degradation. Figure 2, illustrates a brushless cylindrical motor safe operating area is represented. During transients, the motor torque has to be limited to avoid either rotor demagnetization or tooth saturation, so it cannot exceed a given value $T_{em,peak}$. The same for speed, because of shaft bearing or permanent magnet to rotor attachment, the maximum speed has to be limited to $\omega_{abs,max}$. Then gradual degradation arrives, and this is what "nominal" working point ($T_{em,nom}$) presented in datasheets means. In fact the motor torque should be limited while using it for long term operations, in order to bound coil temperature to acceptable values and to limit insulators thermal ageing.

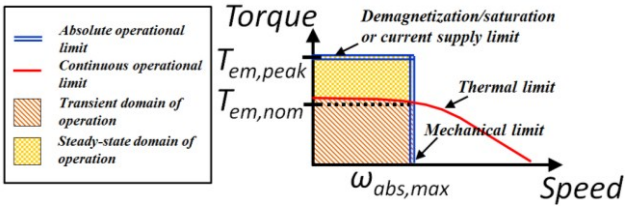

Figure 2: Brushless electric motor safe operating area

One last category of design drivers exists: imperfection parameters. Those components parasitic internal features are likely to impact the component choice itself (for example motor inertia) or on surrounding components sizing (like for the friction losses).

EMA components can be sorted into categories with their own design drivers:

- Rolling mechanism (bearing, rollers/ balls-screw, gears…): transient maximum static load linked to plastic deformation or buckling must not be exceeded, nor the maximum reachable speed linked either to stability/vibration or centrifugal/inertial induced forces. As concerns continuous limits, load/speed must be bounded for thermal/lubrication or fatigue (rolling, structural and wear) purpose. Rolling fatigue can be evaluated by Lundberg-Palmgren formulas [6], derived from bearing application cases. Parasitic effects as friction and transmission compliance can influence the design;
- Sliding mechanism (rod-end, clutch…): a maximum contact pressure is defined for plastic deformation, and then critical transient temperature obtained for a given energy to be dissipated due to friction. Then gradual degradation refers to an amount of wear leading to unacceptable free play within the mechanism. Parasitic effect for rod-ends is friction and the induced flexural torque on housing;
- Static structure (housing): submitted to transient loading that should not lead to a stress higher than yield strength. Then gradual degradation is linked to fatigue (loading, vibrations) and corrosion. Other drivers must be relevant: components geometrical integration and housing thermal properties;

- Electric motor: in addition to aforementioned bounds, transient temperature of the coil should not exceed insulator limit. The main parasitic effect is internal losses (especially joule losses) and rotor inertia resulting to high reflected linear mass for high reduction ratios;
- Power electronics: for transient, the modules safe operating area is defined by its break-down voltage and current/thermic limit. Then gradual degradation depends on thermo-mechanical cycling, that are hard to estimate during the early project phases. Parasitic effects are one more time losses (conduction and switching). The switching frequency is a design parameter which can become critical for high-speed motor design.

3 Models needs and general description

The actuation requirements definition phase can be divided, as illustrated in Figure 3, into various steps based on models:

- Dynamic model: this model may represent specified dynamic performances taking into account components limitations expressed in speed/acceleration non-linearities.
- Load model: load model will mainly be got by aircraft maker flight simulation and aerodynamic calculation. It is complementary to dynamic model because load to position consistency must be ensured.

  Yet, if mission profile filtering (dynamic adaptation) is done separately, a simplified load model can be adjusted on recorded load profile and used for filtering.
- Kinematic model: it will represent integration kinematics movement and its power flow transformation. As represented in Figure 3, it can be used in both calculation causal cases, especially while checking aircraft closed loop stability.
- Analysis models: they represent the core of the toolbox since they will provide ways to evaluate without complete design the effect of design drivers of more electrical technologies summarized in section 2.

First and foremost, the toolbox is dedicated to aircraft makers, but it can also be used by system suppliers as soon as they have got data on load definition and kinematics (mechanism, space envelope…) knowledge.

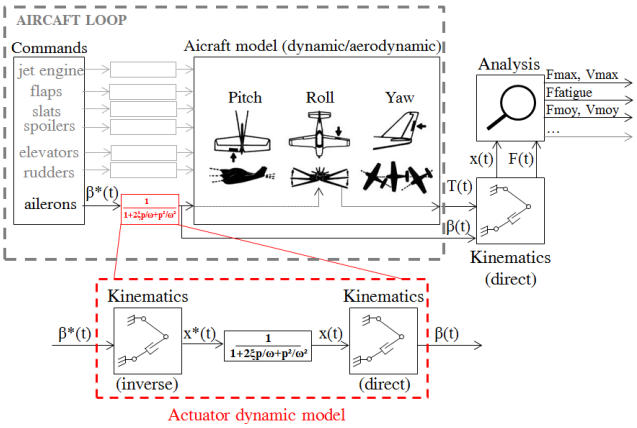

Figure 3: Specifications definition steps and models

The main features of this toolbox enable:

- Comparing consistency/severity of requirements derived from various constraints;
- Adapting (dynamically, or from hinge to actuator power flow) mission profile;
- Extracting important data and/or simplify mission profiles;
- Supporting decision making for architectural and kinematic choices.

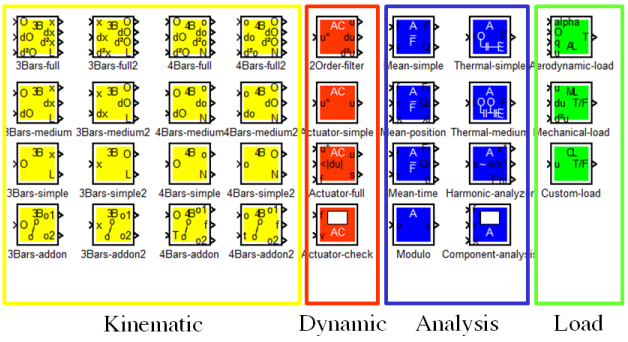

Figure 4: Simulink toolbox library

Models were implemented in Matlab-Simulink library and are regrouped into mentioned subtypes. Not all the blocks presented in Figure 4 will be described in the next part, only ones involved by the presented study cases.

4 Models description and illustration

In this part, the hypothesis and equations describing models will be presented and illustrated on two study cases:

- A long lifetime with low dynamics actuator dedicated to primary flight control used for all illustrations except for dynamic model.
- A high dynamic thrust vector control actuator to explain how to settle and use dynamic model properly.

4.1 Actuator dynamic model

4.1.1 Model description

An actuator cannot respond to a position demand instantaneously and without any alteration. That is why the concepts of time response or frequency response and non-linear limitations have to be introduced and modeled. Time response corresponds to the time when output enters, without going out, into the 95% - 105% of the total realized step.

Frequency response exhibit, within Bode diagram, the magnitude ratio and phase lag between sinusoidal order and actual position. The structure of EMAs' controllers involves a combination of nested loops that can be described by Figure 5 diagram.

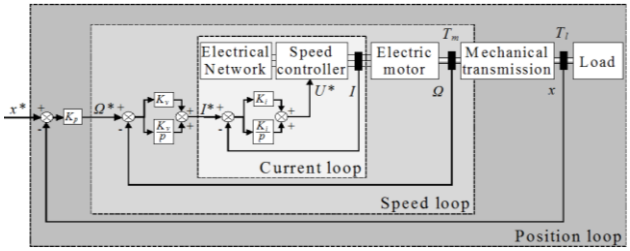

Figure 5: EMA nested control loops [7]

As illustrated, three control loops are implements in common controllers **[8]**, with typical bandwith of: 500Hz-1KHz for current loop, 10Hz-50Hz for speed loop and 2Hz-10Hz for position loop **[9]**. Closed loop performance description with these nested loops appear to be a bit complex at specification level because components dynamic behavior and models are still incompletely known. That is why the EMA model can be approximated by a non-linear second-order transfer function, which is found sufficient as first match.

A second order transfer function and its equivalent differential equation can be derived into the Figure 6 state model representation.

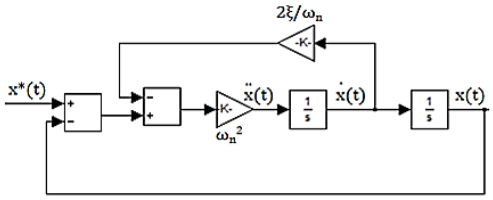

Figure 6: State space representation of a 2nd order

This representation is interesting because all state variables (acceleration, speed and position) can be accessed to introduce further non-linearities/saturations representative of components performances limitations that will be explained later on.

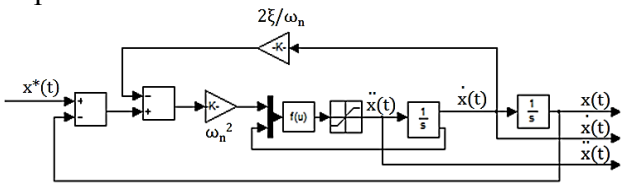

Figure 7: Non-linear 2nd order state space model

The idea is now to link the actuator transient limits to acceleration/speed/position states. Of course, complete simulation with components models and controller (Figure 5) is more realistic, but, one more time, an actuator is not designed at the time when specifications are expressed. So, realistic limitations have to be defined in order to be sure that a physical solution can be obtained.

As demonstrated in **[10]**, the limitations are of two types:

- Motor current/torque limitation impacts high frequency acceleration, with a -40dB/decade slope in the Bode plot of position magnitude;
- Motor maximum speed/voltage limit impacts high frequency speed, and this is represented by a -20dB/decade slope in the same plot.

For a sinusoidal position demand:

$$x^*(t) = x_0 * .\sin(\omega t) \Rightarrow \beta^*(t) \approx \beta_0 * .\sin(\omega t) \qquad \textbf{(1)}$$

Current limitation (I_{max}) hypothesis (neglecting load torque), derived from motor torque (K_m Nm/A constant and J inertia) balance equation, leads to:

$$\beta_l(p) \le \frac{K_m . I_{\max} / J}{\omega^2} \qquad \textbf{(2)}$$

Voltage limitation hypothesis (neglecting the inductive and resistive effects of the motor winidings in comparison with electromotive force), derived from motor DC equivalent electric equation, leads to:

$$\beta_l(p) \le \frac{U_{\max}/K_m}{\omega} \quad (3)$$

So far, the expressed limits correspond to transition between linear and non-linear behavior. But, still in **[10]**, it has been demonstrated that extreme non-linear actuator displacement is slightly bigger, with an adaptation of the aforementioned slope applying a 4/π coefficient:

$$\beta_{nl}(p) \le \frac{4}{\pi}\frac{U_{\max}/K_m}{\omega}; \beta_{nl}(p) \le \frac{4}{\pi}\frac{K_m.I_{\max}/J}{\omega^2} \quad (4)$$

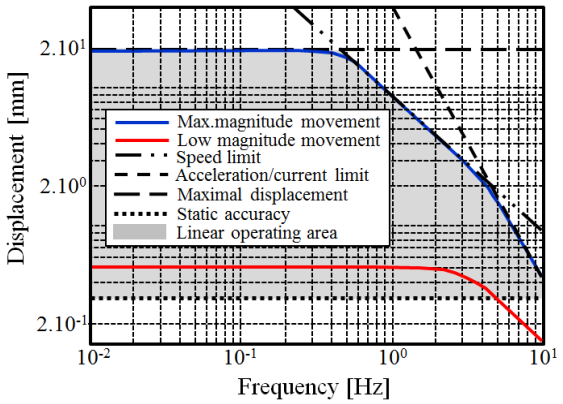

Figure 8: Linear performance limit

As presented in Figure 8, an operating area can be drafted into the frequency graph to represent the limitations.

The presented graph must not be confounded with classical Bode representation of linear system, which gives for a 2nd order model:

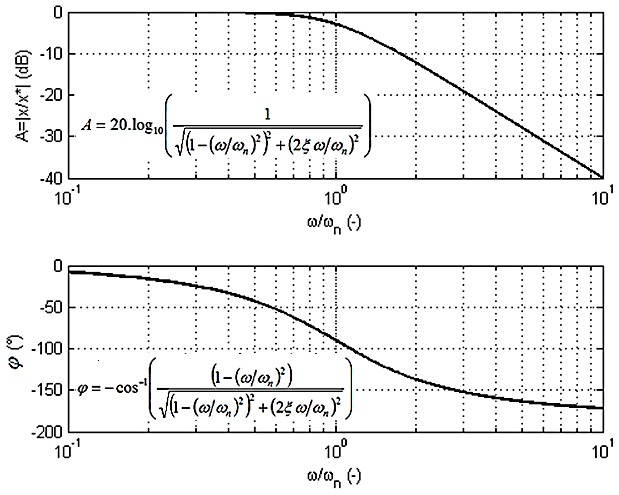

Figure 9: Bode diagram for 2nd order model

The limits impact has been studied for harmonic response only, yet for steps response they will result in an increase of the response time. It can still be interesting to calculate maximum speed and acceleration needed for a given step demand considering linear behavior. First thing first, the second order parameters must be chosen to fulfill specified response time. Taking ξ=0.7 (for minimum response time), then bandwidth can be calculated using the following approximation:

$$\omega_n \approx \frac{2.9}{t_{r,5\%}} \quad (5)$$

Then for a step of magnitude x_0*, the maximum required acceleration will be:

$$\frac{\partial^2 x}{\partial t^2} \le \left.\frac{\partial^2 x}{\partial t^2}\right|_{t=0} = x_0 * .\omega_n{}^2 \quad (6)$$

While maximal speed is (for ξ=0.7):

$$\frac{\partial x}{\partial t} \le \left.\frac{\partial x}{\partial t}\right|_{t=\frac{\tan^{-1}\left(\frac{\sqrt{1-\xi^2}}{\xi}\right)}{\omega_n.\sqrt{1-\xi^2}}} \approx 0{,}46.x_0 * .\omega_n \quad (7)$$

The parameters values of the dynamic model have to validate a wide range of dynamic specifications (harmonic, step response…) which may be specified separately. After comparison, the most severe ones have to be implemented as illustrated in the following example.

4.1.2 Model illustration

To illustrate how the dynamic model can be set, the specification for a thrust vector control actuator summarized in the following tables is treated.

Frequency range	0-0.4Hz	0.4-2Hz	2-3Hz	5-7Hz
Gain (dB)	|G|<0.7	|G|<0.7	|G|<1.5	-5<G<1.6
Phase (°)	-6.5<φ	-36.5<φ	-52<φ	-75<φ

Table 1: Harmonic performance (|β₀*|<0.1°)

Step demand	Response time (tm)	Overshoot
0°→0.5°	0.12s	13%
0°→1.0°	0.15s	9%
1°→4.5°	0.38s	6%
0°→5.5°	0.571s	5%

Table 2: Step response time performance

To fulfill harmonic performance (formulas from Figure 9), and especially phase lag at maximum frequency, $\omega_n \approx 55$rad/s (f=8.7Hz) must be chosen. Then, considering a linear behavior of the actuator for 0.1° magnitude oscillations, the maximal speed will be:

$$\frac{\partial \beta}{\partial t} \le \beta_0 * .\omega_n = \beta_0 * .(2\pi.f) \approx 4.4°/s \quad \textbf{(8)}$$

And acceleration will be:

$$\frac{\partial^2 \beta}{\partial t^2} \le \beta_0 * .\omega_n{}^2 = \beta_0 * .(2\pi.f)^2 \approx 193°/s \quad \textbf{(9)}$$

In comparison, to fulfill step response performance (0.12s minimum response time), only a ω_n=24rad/s (f=4Hz) frequency is required.
Then, to deal with limitation, it will be considered that acceleration limitation mostly influences low magnitude step order, while speed limitation has to be considered for high magnitude step order. Figure 10 and Figure 11 are optimistic behavior hypothesis to determine limitation lower bound.

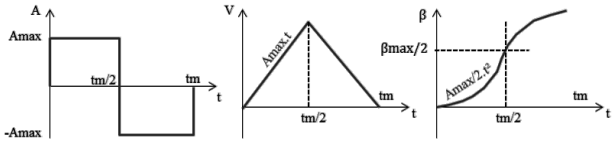

Figure 10: Response to low magnitude step demand

$$A_{\max} = 4.\frac{x_0{}^*}{t_m{}^2}; V_{\max} = A_{\max}.\frac{t_m}{2} \quad \textbf{(10)}$$

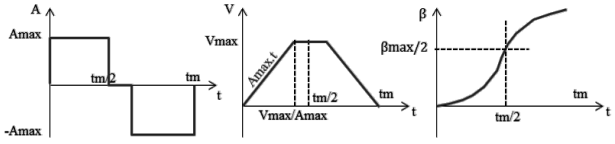

Figure 11: Response to high magnitude step demand

$$V_{\max} = \frac{\left[t_m - \sqrt{t_m{}^2 - 4.\frac{x_0{}^*}{A_{\max}}}\right]}{2}.A_{\max} \quad \textbf{(11)}$$

Applying the formulas, it is found that maximum speed (13.4°/s) and acceleration (178°/s²) derive from 0°→1° step specification.

The general model may be the combination of the most severe performances, in this case harmonic bandwidth and a combination of step/harmonic response limitations (underlined data).

4.2 Load model

4.2.1 Model description

Load model is generally included in aircraft simulator and is part of the aircraft maker's knowledge. Therefore load – position profiles are consistent. Yet if somehow, the specified dynamic differs from the recorded profile (use of hydraulic actuators on-flight measurements, simulation with unadapted sample time), the position profile has to be filtered by using the dynamic model and an equivalent load model has to be defined to link hinge/actuator moment to position.

That is why a typical primary flight control surface load model is presented below. The hinge torque T depends on the dynamic pressure q, wing angle α and the control surface steering angle β **[11]**:

$$T = q.f(\alpha,\beta) \approx q.\left[k_c + k_\alpha.\alpha + k_\beta.\beta\right] \quad \textbf{(12)}$$

The k_i coefficients depend on the air flow properties that may change with wing profile (while opening slats and flaps) or speed conditions.

4.2.2 Model illustration

For the case study, a primary flight control, the k_i parameters had to be adapted depending on the air flow (i.e. dynamic pressure), that is why k_β evolution was studied on different flight phases (same α angle).

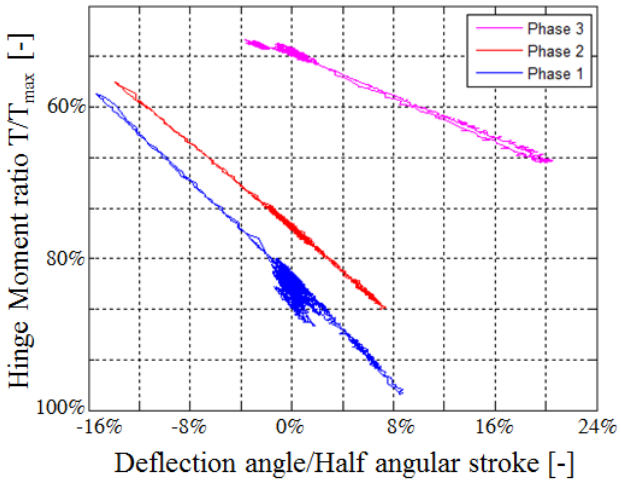

Figure 12: Study of K_β coefficient evolution

Then, defining $k_\beta = f(q)$ function, hinge moment can be validated by comparison with initial data. The obtained model is not perfect but sufficient for most demanding flight phase.

Coefficients needed to be adapted for take-off and landing phases because of slats/flaps impact on air flow.

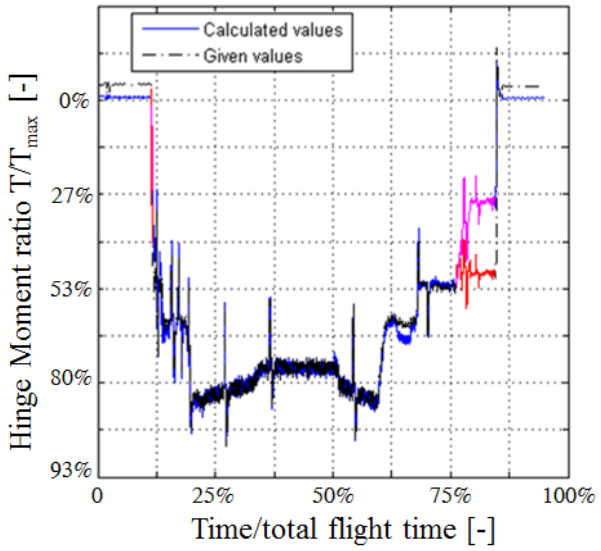

Figure 13: Load model validation

4.3 Linear kinematic model

4.3.1 Model description

Addressing kinematics is an important step for translating hinge properties into actuator requirements. This is obvious when looking back to Figure 3, where it is used many times in both direct and inverse models.

Because of envelope and aerodynamic constraints, actuation systems must be off-centered and surface unfoldment is generally obtained with more or less complex kinematics based on bars lattice. As a consequence, the transmission ratio varies with control surface steering angle.

To give an example of some complex kinematics, one may quote Krueger flaps and Fowler slats. In Figure 14, some diagrams encountered on patents ([12], [13]) are presented.

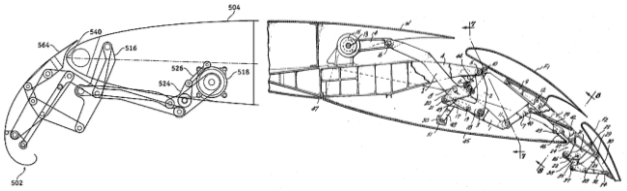

Figure 14: Slats/flaps kinematic patented mechanisms

For such mechanisms, load path and global transmission ratio have to be determined with multi-body kinematics software such as Adams… Yet, some simpler kinematics exists and is often used for primary flight control design: linear 3-bars and rotational 4-bars mechanisms.

As the case study which will be dealt with here is integrated into linear 3-bars kinematics and as only a short part can be dedicated to current paragraph, the 4-bars kinematics based on Freudenstein equations [14] has been implemented in the toolbox but their description is out of scope here.

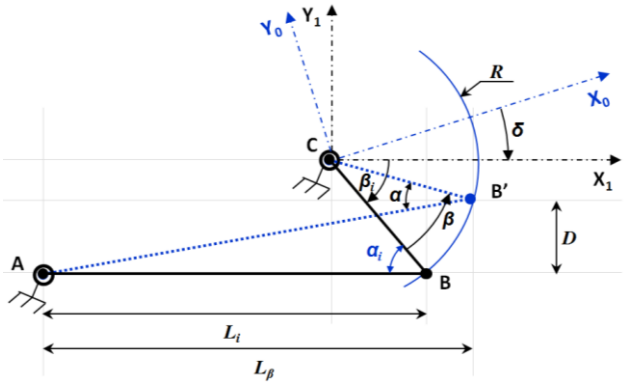

Figure 15: 3-bars mechanism before/after extension

In Figure 15, ABC corresponds to initial configuration, with *AB* representing actuator length, while points '*C*' and '*A*' are pivot axle. Third bar is the aircraft airframe (ground symbol).

Then, the idea is to link the angle α between bars to the steering angle β:

$$\alpha = \beta_i - \beta + \hat{BAB'} \qquad \textbf{(13)}$$

Using tangent value equal to *D*/*L*':

$$\alpha = \beta_i - \beta + \tan^{-1}\left(\frac{R.[\sin(\beta_i) - \sin(\beta_i - \beta)]}{L_i + R.[\cos(\beta_i - \beta) - \cos(\alpha_i)]}\right) \qquad \textbf{(14)}$$

For some geometrical configurations (and especially this case study), the non-linear part can be neglected, leading to:

$$\alpha \approx \beta_i - \beta \qquad \textbf{(15)}$$

Simplifying the reduction ratio expression to:

$$\lambda = \frac{\partial AB/\partial t}{\partial \beta/\partial t} = R.\sin(\alpha) \approx R.\sin(\beta_i - \beta) \qquad \textbf{(16)}$$

4.3.2 Model illustration

Under this hypothesis, a simple initial kinematic optimization can be achieved during specification and will mostly consist in choosing the right *R* and α_i (or β_i) initial parameters, depending on preliminary sizing feedback on most important sizing criteria. Graphically, it means moving operating window in Figure 16.

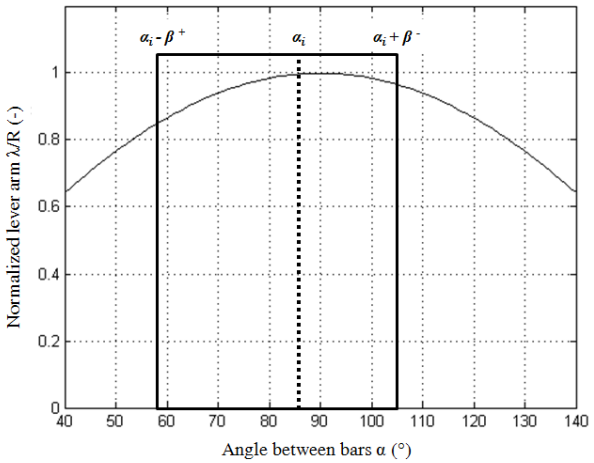

Figure 16: Reduction ratio operating window

4.4 Mechanical analysis model

4.4.1 Model description

The first mechanical analysis will consist in extracting extreme speed and force values which induce rapid degradation phenomena. For gradual degradation phenomena, the idea is to estimate, at load mission profile level, cumulated rolling fatigue/wear…, by different means:

- Integrating wear (j=1; k=1) or rolling fatigue (j=3; k=1) on time intervals and different thread/tooth sides (Q^+, Q^-).

$$Q_i^+ = \int_{t_{i-1}}^{t_i} \left|F_{pr} + 0.64.F(t)\right|^j .\left(F(t) \geq -2.8.F_{pr}\right)|V|^k .dt$$
$$Q_i^- = \int_{t_{i-1}}^{t_i} \left|F_{pr} - 0.36.F(t)\right|^j .\left(F(t) \leq 2.8.F_{pr}\right)|V|^k .dt \quad \textbf{(17)}$$

- Making the integration on position intervals instead of time (similar formulas).

Previous formulas are derived from sphere/plane Hertz contact theory and equivalent non-linear stiffness formula.

For non-preloaded (F_{pr}=0→F_{tr}=0) devices, or when contact is lost ($|F| \geq 2.8F_{pr}=F_{tr}$), formulas expression change.

$$Q_i^{\pm} = \int_{t_{i-1}}^{t_i} |F(t)|^j .\left(\pm F(t) \geq F_{tr}\right)|V|^k .dt \quad \textbf{(18)}$$

4.4.2 Model illustration

Applying the formulas to study case nominal flight mission profile, an analysis according to time and stroke can be derived as represented Figure 17.

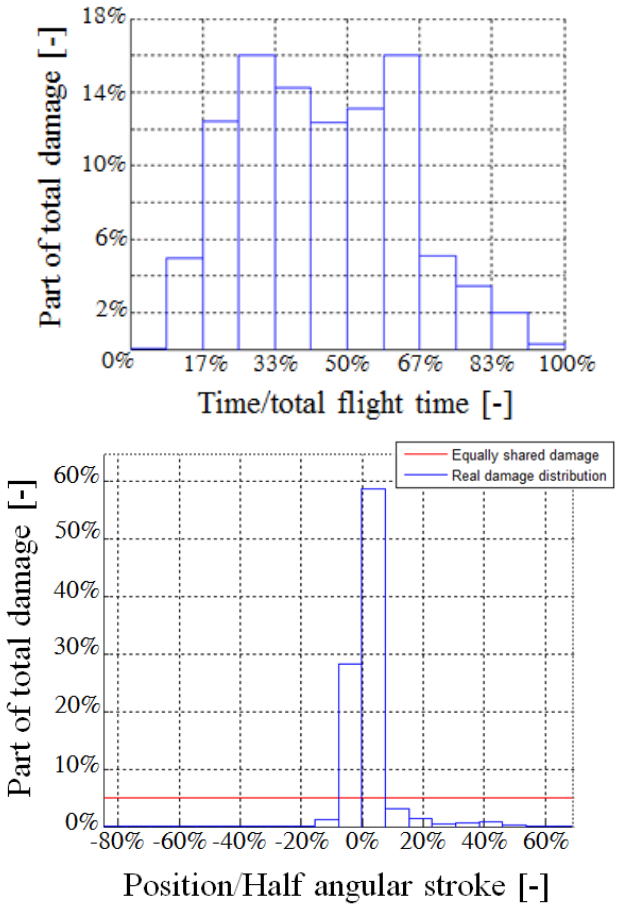

Figure 17: Rolling fatigue distribution

Considering non-preloaded mechanical transmission parts, it is noticed that rolling fatigue mainly occurs during cruise and impacts a very short portion of total stroke. As shown in **[15]**, an equivalent profile considering 1.6% of the half stroke and a 0.45Hz sinusoidal movement under ½ F_{max} generates the same degradation and simplifies specification, design and test.

4.5 Tools for architecture choice

4.5.1 Tools description

Actuator specifications can provide performance requirements just like architecture. Therefore, early technology evaluation, especially centered on motor-reducer choices will be helpful. As transmission ratio has not been chosen yet, it will be interesting to compare non-variable power values such as:

- Peak power Pm= Fmax.Vmax;
- Nominal power $P_n=F_{rms}.V_{max}$, where RMS load is the maximum filtered square load representative of the motor joule losses (will be detailed lately).
- …

Considering a nut-screw pitch value of 5mm and the maximum reduction ratio reachable with each reducer technologies (2 spur gear stages reducer N≤25:1, epicyclic reducer N≤100:1 and harmonic reducer N≤300:1), it is possible to draw a technology selection graph based on scaling laws **[16]**, as in Figure 18.

Depending on the chosen representation, motor sizing design drivers change. That is why this selection phase must rely on previous knowledge, and has to be used with care. For example, peak power graph supposes that motor is sized for max torque and speed (no thermal or inertial limitations) and inertia load is neglected.

That is why a very important question arises: is inertia additional load negligible? One way to answer to, is to compare peak power to power rate ($P_r=A_{max}.F_{max}$), as in Figure 20, also on basis of scaling laws. If part of max torque used to accelerate inertia is low, the hypothesis is verified.

A method developed by Van de Straete **[17]** consists in adapting the mechanical torque/ speed equations to motor output shaft by introducing a particular reduction ratio combining transmission ratio N and motor inertia J_m:

$$\frac{T_{em,\max}}{\sqrt{J_m}} \geq \sqrt{J_m}.N.a(t) + \frac{1}{N\sqrt{J_m}}F(t) = n^*.a(t) + \frac{F(t)}{n^*} \qquad \sqrt{J_m}\,\omega_{abs,\max} \geq \sqrt{J_m}N.V(t) = n^*.V(t) \qquad \textbf{(19)}$$

Those quantities are renamed as $T^*(n^*)$ normalized load and $\Omega^*(n^*)$ normalized speed. Then a given working point can be represented by a curve (depending on n^* adaptation) into the T^*-Ω^* graph.

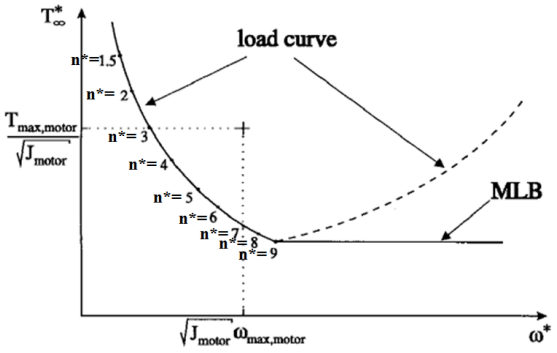

Figure 19: Van de Straete diagram [17]

For a complete mission profile, maximum speed point must be kept for its severity, then, all the other points must be compared in the (1/|acceleration|) vs. (1/|load|) graph, keeping the Pareto front. Further mathematical analysis considering saturation limit (part where Minimum Lower Bound (MLB) applies) has to be processed to decrease the number of potentially severe points. The technique will not be discussed here.

4.5.2 Tools illustration

Figure 18 and Figure 20 illustrate the use of such analysis criteria on primary flight control actuation system.

For a 2kW peak power and 70mm/s maximum speed rate, high speed motor coupled to a spur-gear reducer, seems to be a suitable architecture.

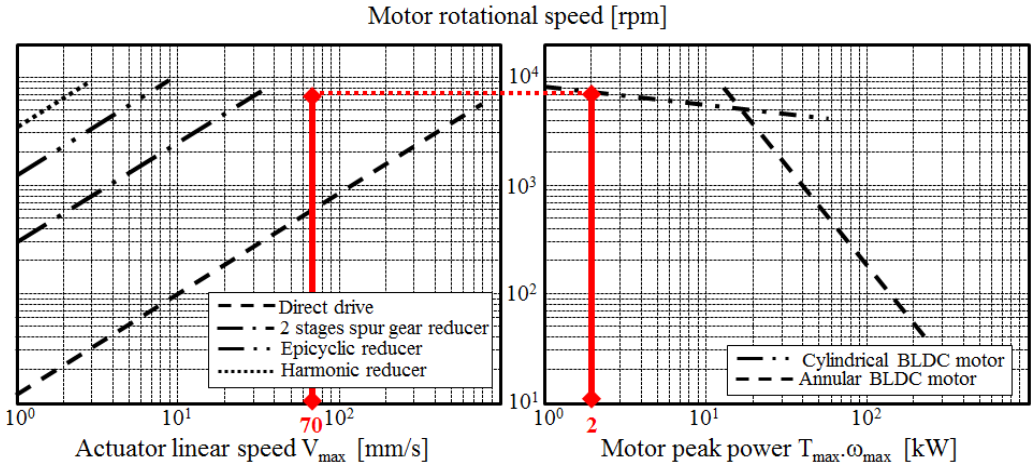

Figure 18: Technology early choices

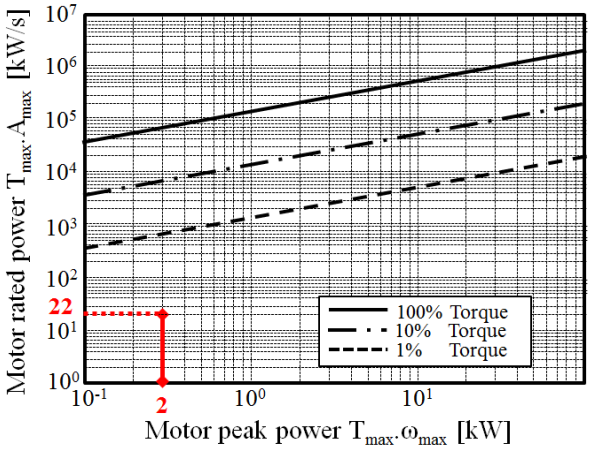

Figure 20: Power – power rate diagram

Inertia load represents less than 1% of motor maximum torque, so it can be neglected, and mission profile representing inertial constraint is not necessary.

4.6 Thermal analysis model

4.6.1 Model description

EMA technologies are more stressed by thermal effects than servo hydraulic actuator technologies, needing additional requirements. To perform thermal analysis at mission profile level, motor thermal model must be defined in a simple way in order to filter the copper losses or at least one proportional representative value, the root mean squared load, F_{RMS}.

$$\sqrt{P_J} \propto F_{RMS} = \sqrt{\frac{1}{T}\int_0^T F_{filtered}(t)^2\,dt} \qquad \textbf{(20)}$$

The filtering models can be made of one or two bodies in order to represent transient thermal evolution of electrical motors:

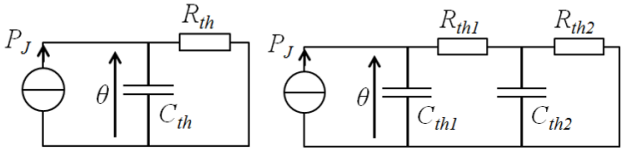

Figure 21: Motor thermal models

Where R_{th1} and C_{th1} are respectively copper-iron conductive resistance and copper thermal capacity, while R_{th2} and C_{th2} stands for iron-air convective resistance and iron thermal capacity.
For one body model, thermal resistance R_{th} and capacity C_{th} are a combination of previous parameters.

Related transfer functions are the following:

$$G(p) = \frac{F^2{}_{filtered}(p)}{F^2(p)} = \frac{1}{1+(R_{th}C_{th})p} = \frac{1}{1+\tau_{th}p} \qquad \textbf{(21)}$$

For one body model and, for two bodies:

$$G(p) = \frac{1+\left(\frac{\tau}{k_R(1+1/k_R)^2(1+1/k_C)}\right)p}{1+\left(\frac{\tau.(k_Rk_C+k_C+1)}{k_Ck_R(1+1/k_R)(1+1/k_C)}\right)p+\left(\frac{\tau^2}{k_Rk_C(1+1/k_R)^2(1+1/k_C)^2}\right)p^2} \qquad \textbf{(22)}$$

$$k_R = \frac{R_{th1}}{R_{th2}};\quad k_C = \frac{C_{th1}}{C_{th2}};\quad \tau = (R_{th1}+R_{th2})(C_{th1}+C_{th2})$$

Generally, motor time constant is 10-20min.

4.6.2 Model illustration

As presented in Figure 22, and even with very different parameters involved in the thermal model ($k_R \in [1/4;1]$ and $k_C \in [1/4;1/2]$), overheat appears during cruise phase. The total profile has been completed with 50% additional rest time corresponding to on-ground preparation (refueling, passengers' boarding / disembarkation…).
As for fatigue, an equivalent simpler step stall load (40% max load) of cruise duration will lead to the same overheat.

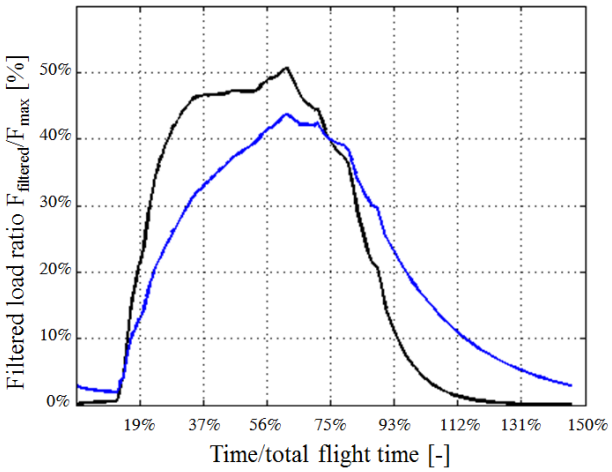

Figure 22: Motor extreme thermal behavior

Conclusion

The definition of EMAs performance requirements is a complex task because of its high coupling with aircraft closed loop stability and aerodynamic models embedded in the global simulator. This knowledge possessed by airplane makers must be partitioned for confidentiality and competition reasons to the manufacturers themselves. That is why the models library was designed to help the engineer with requirements formulation task.
An early analysis highlights the most severe stated performances and shortens shared mission profiles by formulating equivalent simplified ones. Most important EMAs' limitations have been listed to have a complete, standard and simpler requirement list for system supplier, which better targets technology needs.
Finally, actuator integrated kinematics (3-bars linear model) was introduced with few suggestions and remarks on optimization and integration.
All this will limit information exchanges and dissemination, and simplify the supplier's further task.

References

[1] Todeschi M. Airbus - EMAs for flight actuation systems – perspectives. *Proc international conference on Recent Advances in Aerospace Actuation Systems and Components (RAASC)*, Toulouse, pp. 1-8, 2010.

[2] Actuation 2015, http://www.actuation2015.eu/.

[3] Van Den Bossche D. The A380 primary flight control actuation system. *Proc RAASC international conference*, Toulouse, pp. 1-4, 2001.

[4] Grand S. & al. Electromechanical actuators design for thrust vector control. *Proc RAASC international conference*, Toulouse, pp. 21-27, 2004.

[5] Dée G. & al. An electrical thrust vector control system with dynamic force feedback. *Proc RAASC international conference*, Toulouse, pp. 75-79, 2007.

[6] G. Lundberg & al. *Acta politechnica - mech*. Eng. series, vol. 1, n°3, 1947.

[7] Hospital F. Conception préliminaire des actionneurs électromécaniques basée sur les modèles: lois d'estimations et règles de conception pour la transmission de puissance mécanique. *Thesis report*, Toulouse, 2012.

[8] Grellet G. *Actionneurs électriques : principes, modèles, commandes*. Eyrolles, 1989.

[9] Ellis G. *Control system design guide*. Elsevier, 2004.

[10] Webb J. &. al. Predicting dynamic performance limits for servosystems whith saturating nonlinearities. *NASA technical report 1488*, 1979.

[11] Annaz F. Fundamental design concepts in multi-lane smart electromechanical actuators. *Smart materials and structures*, vol. 14, pp. 1227-1238, 2005.

[12] Cole J. Airfoil flap conical extension mechanism. *Patent US4172575*, 1979.

[13] Sakurai S. &. al. High-positioned 3-position variable camber Krueger flap. *Patent EP2626295*, 2013.

[14] Freudenstein F. Approximate synthesis of four-bar linkage. *Proc ASME*, vol. 77, n°18, pp. 853-861, 1955.

[15] Jaafar A. Traitement de la mission et des variables environnementales et intégration au processus de conception systémique. *Thesis report*, Toulouse, 2011.

[16] Liscouet J. &. al. Preliminary design of electro-mechanical actuators. Proc of the Institution of Mechanical Engineers, Journal of Aerospace, 2012.

[17] Van de Straete H. &. al. Servo motor selection criterion for mechatronics application. *ASME transactions on mechatronics,* vol. 3, pp. 43-50, 1998.

Contact Author Email Address

aurelien.reysset@insa-toulouse.fr
marc.budinger@insa-toulouse.fr

Acknowledgements

The work presented was partly funded by the European ACTUATION 2015 project (Modular Electro Mechanical Actuators for ACARE 2020 aircraft and helicopters).

Copyright Statement